Carboxylate- and Phosphate Ester-Bridged Dimagnesium(II), Dizinc(II), and Dicalcium(II) Complexes. Models for Intermediates in Biological Phosphate Ester Hydrolysis

Joanne W. Yun, Tomoaki Tanase,† and Stephen J. Lippard*

Department of Chemistry, Massachusetts Institute of Technology, Cambridge, Massachusetts 02139

Received July 25, 1996[⊗]

Carboxylate-bridged dimagnesium(II) complexes were synthesized and characterized by employing the dinucleating ligand XDK, where H_2XDK is *m*-xylylenediamine bis(Kemp's triacid imide). The reaction of 1 or 2 equiv of sodium diphenyl phosphate with $[Mg_2(XDK)(CH_3OH)_4(H_2O)_2(NO_3)](NO_3)$, **1**$(NO_3)$, afforded $[Mg_2(XDK)\{\mu\text{-}\eta^2\text{-}(PhO)_2PO_2\}(CH_3OH)_3(H_2O)(NO_3)]\cdot 3CH_3OH$ (**2**·$3CH_3OH$) and $[Mg_2(XDK)\{\mu\text{-}\eta^2\text{-}(PhO)_2PO_2\}\{\eta^1\text{-}(PhO)_2PO_2\}(CH_3OH)_3(H_2O)]\cdot CH_3OH$ (**3**·CH_3OH), respectively. These are the first structurally characterized phosphate ester-bridged dimagnesium(II) complexes. The reaction of **1** with 1 equiv of bis(4-nitrophenyl) hydrogen phosphate resulted in protonation of one of the carboxylate ligands and liberation of one magnesium(II) ion to give $[Mg(HXDK)_2(H_2O)_2]$ (**4**), an octahedral complex containing two short, low barrier intramolecular OH···O hydrogen bonds. The phosphate ester exchange rate of free and bound diphenyl phosphate in **3** in methanol solution was measured by variable-temperature $^{31}P\{^1H\}$ NMR spectroscopy and compared to that of structurally analogous dizinc(II), $[Zn_2(XDK)\{\mu\text{-}\eta^2\text{-}(PhO)_2PO_2\}\{\eta^1\text{-}(PhO)_2PO_2\}(CH_3OH)_2(H_2O)]$ (**5**), and dicalcium(II), $[Ca_2(XDK)\{\mu\text{-}\eta^2\text{-}(PhO)_2PO_2\}\{\eta^1\text{-}(PhO)_2PO_2\}(CH_3OH)_3(H_2O)]\cdot CH_3OH$, (**6**·$CH_3OH$), complexes. The synthesis and structural characterization of **6** is presented, along with a discussion of the differences between the carboxylate- and phosphate ester-bridged dimagnesium(II), dizinc(II), and dicalcium(II) centers. Crystallographic data are as follows. **1**(NO_3): monoclinic, $P2_1/c$, $a = 11.240(3)$ Å, $b = 13.019(2)$ Å, $c = 30.208(7)$ Å, $\beta = 99.11(1)°$, $V = 4365(2)$ Å^3, $Z = 4$, $R = 0.045$, and $R_w = 0.054$ for 5021 independent reflections with $I > 3\sigma(I)$. **2**·$3CH_3OH$: monoclinic, $P2_1/c$, $a = 16.611(5)$ Å, $b = 16.059(6)$ Å, $c = 21.930(9)$ Å, $\beta = 93.34(6)°$, $V = 5840(4)$ Å^3, $Z = 4$, $R = 0.069$, and $R_w = 0.085$ for 3759 independent reflections with $I > 2\sigma(I)$. **3**·CH_3OH: monoclinic, $P2_1/n$, $a = 18.912(4)$ Å, $b = 16.254(2)$ Å, $c = 21.646(5)$ Å, $\beta = 112.26(2)°$, $V = 6158(2)$ Å^3, $Z = 4$, $R = 0.060$, and $R_w = 0.072$ for 5184 independent reflections with $I > 3\sigma(I)$. **4**: monoclinic, $P2_1/n$, $a = 15.210(5)$ Å, $b = 15.772(3)$ Å, $c = 13.093(3)$ Å, $\beta = 96.35(3)°$, $V = 3122(1)$ Å^3, $Z = 2$, $R = 0.069$, and $R_w = 0.070$ for 1840 independent reflections with $I > 2\sigma(I)$. **6**·CH_3OH: monoclinic, $P2_1/n$, $a = 16.5471(3)$ Å, $b = 24.3415(6)$ Å, $c = 16.5865(3)$ Å, $\beta = 104.2530(10)°$, $V = 6475.1(2)$ Å^3, $Z = 4$, $R = 0.053$, and $wR^2 = 0.142$ for 7858 independent reflections with $I > 2\sigma(I)$.

Introduction

Magnesium ion is an indispensable cofactor in biology. It participates in many important biochemical transformations, including the hydrolysis of phosphate ester bonds. The carboxylate-bridged dinuclear magnesium(II) unit, $\{Mg_2(O_2CR)\}^{3+}$, is emerging as a ubiquitous structural motif in many phosphate ester-processing enzymes. These magnesium-dependent enzymes include the Klenow fragment of DNA polymerase I from *Escherichia coli*,[1] ribonuclease H of HIV-1 reverse transcriptase,[2] rat DNA polymerase β,[3,4] fructose-1,6-bisphosphatase,[5,6] inositol monophosphatase,[7] and inositol polyphosphate 1-phosphatase,[8] which have all been structurally characterized to reveal a carboxylate-bridged dimetallic active site center. These metalloenzymes comprise a rapidly growing class of enzymes postulated to utilize a two-metal-ion mechanism for phosphate ester hydrolysis. Their dimagnesium(II) centers are believed to serve several important functions, including (i) binding, orienting, and activating the substrate, (ii) modulating the pK_a of the incoming nucleophile, (iii) stabilizing the transition state, and (iv) facilitating product release.[1] Furthermore, studies of catalytic RNA systems have suggested a similar requirement for divalent metal ions,[9] and an analogous two-metal-ion mechanism has been proposed for the ribozymes.[10]

We are particularly interested in studying the manner by which phosphatases employ a carboxylate-bridged dimagnesium(II) center to catalyze the cleavage of phosphate ester bonds. Our approach to investigating the underlying structural and mechanistic principles is to prepare and characterize small molecule inorganic complexes that contain a carboxylate-bridged dimagnesium(II) core to mimic the biological active sites. Despite the importance of such dimagnesium(II) centers in the active sites of metalloenzymes, examples of structurally characterized dimagnesium(II) carboxylate complexes are extremely rare. A search of the Cambridge Structural Database revealed

† Permanent address: Department of Chemistry, Faculty of Science, Nara Women's University, Nara 630, Japan.

⊗ Abstract published in *Advance ACS Abstracts,* December 1, 1996.

(1) Beese, L. S.; Steitz, T. A. *EMBO J.* **1991**, *10*, 25−33.
(2) Davies, J. F.; Hostomska, Z.; Hostomsky, Z.; Jordan, S. R.; Matthews, D. A. *Science* **1991**, *252*, 88−95.
(3) Davies, J. F.; Almassy, R. J.; Hostomska, Z.; Ferre, R. A.; Hostomsky, Z. *Cell* **1994**, *76*, 1123−1133.
(4) Pelletier, H.; Sawaya, M. R.; Kumar, A.; Wilson, S. H.; Kraut, J. *Science* **1994**, *264*, 1891−1903.
(5) Xue, Y.; Huang, S.; Liang, J.-Y.; Zhang, Y.; Lipscomb, W. N. *Proc. Natl. Acad. Sci. U.S.A.* **1994**, *91*, 12482−12486.
(6) Villeret, V.; Huang, S.; Zhang, Y.; Lipscomb, W. N. *Biochemistry* **1995**, *34*, 4307−4315.
(7) Bone, R.; Frank, L.; Springer, J. P.; Atack, J. R. *Biochemistry* **1994**, *33*, 9468−9476.
(8) York, J. D.; Ponder, J. W.; Chen, Z.-W.; Mathews, F. S.; Marjerus, P. W. *Biochemistry* **1994**, *33*, 13164−13171.
(9) Piccirilli, J. A.; Vyle, J. S.; Caruthers, M. H.; Cech, T. R. *Nature* **1993**, *361*, 85−88.
(10) Steitz, T. A.; Steitz, J. A. *Proc. Natl. Acad. Sci. U.S.A.* **1993**, *90*, 6498−6502.

S0020-1669(96)00894-4 CCC: $12.00

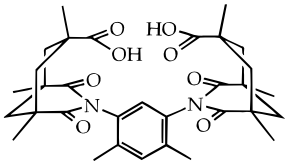

Figure 1. Sketch of the H_2XDK ligand.

only one discrete dinuclear magnesium(II) structure, dimagnesium(II) *o*-phenylenediaminetetraacetate, $[Mg_2(C_{14}H_{12}N_2O_8)(H_2O)_6]$.[11] In the presence of simple carboxylates such as formate, magnesium(II) ions tend to form polymers.[12]

In order to avoid such polymeric structures, we employed the dinucleating ligand XDK (Figure 1), where H_2XDK is *m*-xylylenediamine bis(Kemp's triacid imide).[13,14] This ligand has two convergent carboxylate groups, positioned about 3 Å apart, and is useful for assembling discrete dimetallic units. H_2-XDK has recently been employed in the preparation of a variety of carboxylate-bridged homo-[15−21] and heterodimetallic[22−24] complexes. The present work describes the preparation and characterization of the desired discrete carboxylate-bridged dinuclear magnesium(II) complexes with the XDK ligand. We report the synthesis and structural characterization of carboxylate- and phosphodiester-bridged dimagnesium(II) complexes as potential models for magnesium-activated phosphate ester-processing enzymes. The phosphate ester exchange process of a bis(phosphato)dimagnesium(II)−XDK complex together with its dicalcium(II)− and dizinc(II)−XDK analogs is also presented. A preliminary account of this work has appeared.[25]

Experimental Section

General Procedures. All experiments were carried out in air using commercially available reagents and solvents. The H_2XDK and $[Zn_2(XDK)\{\mu\text{-}\eta^2\text{-}(PhO)_2PO_2\}\{\eta^1\text{-}(PhO)_2PO_2\}(CH_3OH)_2(H_2O)]$ (**5**) compounds were prepared as described previously.[14,24] ^{1}H and ^{31}P{^{1}H} NMR spectra were obtained on Varian XL-300 or Varian UNITY300 spectrometers. ^{31}P{^{1}H} NMR spectra were measured at 121.4 MHz with 85% H_3PO_4 as an external reference. VT-NMR data for **3** and **5** were fit with the program DNMR.[26] Infrared spectra were recorded on a Bio-Rad FTS7 Fourier transform instrument. Conductivity measurements were carried out at 21 °C in methanol with a Fisher Scientific conductivity bridge, Model 9-326, with a platinum-black electrode. Molar conductivities (Ω^{-1} cm^2 mol^{-1}) were derived from the slopes of a conductivity (Ω^{-1} cm^{-1}) vs concentration (mol cm^{-3}) plot. The assignment of the electrolyte type was determined by reference to the molar conductivity of $Bu_4N(PF_6)$ in methanol.

Preparation of $[Mg_2(XDK)(CH_3OH)_4(H_2O)_2(NO_3)](NO_3)$, 1($NO_3$). A methanolic solution (5 mL) of $Mg(NO_3)_2\cdot 6H_2O$ (176 mg, 0.689 mmol) was added to a solution of H_2XDK (200 mg, 0.344 mmol) and NaOH (0.689 mmol, 0.5 M in MeOH) in methanol (5 mL). The mixture was stirred at room temperature for 30 min. The solvent was removed and the residue dried under vacuum. The dried white powder was treated with excess pyridine (5 mL) in chloroform (10 mL), and the insoluble salt contaminants were removed by filtration. The py/$CHCl_3$ filtrate containing the desired complex was placed under vacuum to remove the solvents. The dried sample was then redissolved in methanol and filtered through Celite, and vapor diffusion of ethyl ether afforded colorless crystals in 72% yield (227 mg, 0.248 mmol). The crystals were washed with Et_2O and dried under vacuum. ^{1}H NMR, 300 MHz (CD_3OD): δ 1.19 (s, 6 H), 1.24 (m, 4 H), 1.29 (s, 12 H), 1.61 (d, 2 H, J = 13 Hz), 1.93 (s, 6 H), 2.15 (d, 2 H, J = 13 Hz), 2.85 (d, 4 H, J = 12 Hz), 7.20 (s, 1 H), 7.36 (s, 1 H). IR (Nujol): 3387 (br), 1714 (m), 1680 (s), 1635 (m) (XDK), 1505 (m), 1301 (m), 1191 (m), 1024 (m), 954, 889, 884, 764 cm^{-1}. Anal. Calcd for $C_{36}H_{58}N_4O_{20}Mg_2$: C, 47.23; H, 6.39; N, 6.12. Found: C, 46.96; H, 6.44; N, 6.14.

Preparation of $[Mg_2(XDK)\{\mu\text{-}\eta^2\text{-}(PhO)_2PO_2\}(CH_3OH)_3(H_2O)(NO_3)]\cdot 3CH_3OH$, 2·3$CH_3OH$. A methanolic solution (5 mL) of $Mg(NO_3)_2\cdot 6H_2O$ (44 mg, 0.172 mmol) was added to a solution of H_2XDK (50 mg, 0.0861 mmol) and NaOH (0.172 mmol, 0.5 M in MeOH) in methanol (5 mL) and stirred for 20 min. A methanolic solution (2 mL) of diphenyl hydrogen phosphate (HDPP) (21.5 mg, 0.0861 mmol) and NaOH (0.0861 mmol, 0.5 M in MeOH) was then added. The combined solution was stirred for 30 min, and the solvent was removed under vacuum. The dried compound was redissolved in methanol and filtered, and vapor diffusion of ethyl ether into the solution gave crystalline material. The crystals were collected and treated with excess pyridine (3 mL) in chloroform (5 mL). The salt contaminants were removed by filtration, and the py/$CHCl_3$ filtrate containing the complex was placed under vacuum to remove the solvents. The dried sample was redissolved in methanol, and vapor diffusion of ethyl ether afforded single X-ray quality crystals of **2**·3CH_3OH in 36% yield (36 mg, 0.0313 mmol). ^{1}H NMR, 300 MHz (CD_3OD): δ 1.20 (m, 4 H), 1.23 (s, 6 H), 1.26 (s, 12 H), 1.56 (d, 2 H, J = 13 Hz), 1.90 (s, 6 H), 2.09 (d, 2 H, J = 13 Hz), 2.90 (d, 4 H, J = 14 Hz), 7.02 (m, 2 H), 7.12 (m, 5 H), 7.22 (m, 4 H), 7.45 (s, 1 H). ^{31}P{^{1}H} NMR, 121.4 MHz (CD_3OD): δ −15.46 (s). IR (Nujol): 3472 (br), 1720 (m), 1681 (s), 1619 (m) (XDK), 1317, 1263, 1231, 1194, 1128 (m), 1033, 929 (m), 887, 852, 779, 757, 688 cm^{-1}. Elemental analysis samples were dried under vacuum at 90 °C for 12 h. Anal. Calcd for $C_{47}H_{62}N_3O_{19}Mg_2P$ (**2**): C, 53.63; H, 5.94; N, 3.99. Found: C, 53.22; H, 5.60; N, 4.13.

Preparation of $[Mg_2(XDK)\{\mu\text{-}\eta^2\text{-}(PhO)_2PO_2\}\{\eta^1\text{-}(PhO)_2PO_2\}(CH_3OH)_3(H_2O)]\cdot CH_3OH$, 3·$CH_3OH$. A methanolic solution (2 mL) of HDPP (43 mg, 0.172 mmol) and NaOH (0.172 mmol, 0.5 M in MeOH) was added to a solution of **1** in methanol (5 mL). The mixture was stirred at room temperature for 30 min. The solvent was removed under vacuum. The dried powder was dissolved in methanol, and vapor diffusion of ethyl ether gave crystalline material. The crystals were collected and dried under vacuum and then treated with excess pyridine (3 mL) in chloroform (5 mL), and any salt contaminants were removed by filtration. The py/$CHCl_3$ filtrate containing the complex was placed under vacuum to remove the solvents. The dried sample was then redissolved in methanol and filtered through Celite, and vapor diffusion of ethyl ether afforded colorless crystals of **3**·CH_3OH in 32% yield (35 mg, 0.028 mmol). The crystals were washed with Et_2O and dried under vacuum. ^{1}H NMR, 300 MHz (CD_3OD): δ 1.18 (d, 4 H, J = 14 Hz), 1.23 (s, 6 H), 1.26 (s, 12 H), 1.56 (d, 2 H, J = 13 Hz), 1.90 (s, 6 H), 2.09 (d, 2 H, J = 13 Hz), 2.91 (d, 4 H, J = 13 Hz), 7.03 (m, 4 H), 7.16 (m, 8 H), 7.24 (m, 9 H), 7.47 (s, 1 H). ^{31}P{^{1}H} NMR, 121.4 MHz (CD_3OD): δ −9.14 (s), −15.45 (s). IR (Nujol): 3468 (br), 1717 (m), 1679 (s), 1633 (m), 1597 (m) (XDK), 1288, 1251, 1205 (m), 1135 (m), 1025, 932 (m), 893, 852, 761, 683 cm^{-1}. Samples for elemental analysis were dried under vacuum at 90 °C for 12 h. Anal. Calcd for $C_{59}H_{72}N_2O_{20}Mg_2P_2$ (**3**): C, 57.16; H, 5.85; N, 2.26. Found: C, 56.76; H, 5.47; N, 2.45.

Preparation of $[Mg(HXDK)_2(H_2O)_2]$, 4. Method 1. One equiva-

(11) Nakasuka, N.; Shiro, M. *Acta. Cryst.* **1989**, *C45*, 1487−1490.
(12) Malard, C.; Pezerat, H.; Herpin, P.; Toledano, P. *J. Solid State Chem.* **1982**, *41*, 67−74.
(13) Kemp, D. S.; Petrakis, K. S. *J. Org. Chem.* **1981**, *46*, 5140−5143.
(14) Rebek, J., Jr.; Marshall, L.; Wolak, R.; Parris, K.; Killoran, M.; Askew, B.; Nemeth, D.; Islam, N. *J. Am. Chem. Soc.* **1985**, *107*, 7476−7481.
(15) Goldberg, D. P.; Watton, S. P.; Masschelein, A.; Wimmer, L.; Lippard, S. J. *J. Am. Chem. Soc.* **1993**, *115*, 5346−5347.
(16) Watton, S. P.; Masschelein, A.; Rebek, J., Jr.; Lippard, S. J. *J. Am. Chem. Soc.* **1994**, *116*, 5196−5205.
(17) Tanase, T.; Yun, J. W.; Lippard, S. J. *Inorg. Chem.* **1995**, *34*, 4220−4229.
(18) Tanase, T.; Lippard, S. J. *Inorg. Chem.* **1995**, *34*, 4682−4690.
(19) Hagen, K. S.; Lachicotte, R.; Kitaygorodskiy, A.; Elbouadili, A. *Angew. Chem., Int. Ed. Engl.* **1993**, *32*, 1321−1324.
(20) Hagen, K. S.; Lachicotte, R.; Kitaygorodskiy, A. *J. Am. Chem. Soc.* **1993**, *115*, 12617−12618.
(21) Herold, S.; Pence, L. E.; Lippard, S. J. *J. Am. Chem. Soc.* **1995**, *117*, 6134−6135.
(22) Tanase, T.; Watton, S. P.; Lippard, S. J. *J. Am. Chem. Soc.* **1994**, *116*, 9401−9402.
(23) Watton, S. P.; Davis, M. I.; Pence, L. E.; Rebek, J., Jr.; Lippard, S. J. *Inorg. Chim. Acta* **1995**, *235*, 195−204.
(24) Tanase, T.; Yun, J. W.; Lippard, S. J. *Inorg. Chem.* **1996**, *35*, 3585−3594.
(25) Yun, J. W.; Tanase, T.; Pence, L. E.; Lippard, S. J. *J. Am. Chem. Soc.* **1995**, *117*, 4407−4408.
(26) Sandstrom, J. *Dynamic NMR Spectroscopy*; Academic Press Inc.: London, 1982.

Table 1. Crystallographic and Experimental Data for **1**(NO_3), **2**·3CH_3OH, **3**·CH_3OH, and **4**

	1(NO_3)	**2**·3CH_3OH	**3**·CH_3OH	**4**
formula	$C_{36}H_{58}N_4O_{20}Mg_2$	$C_{50}H_{74}N_3O_{22}Mg_2P$	$C_{60}H_{76}N_2O_{21}Mg_2P_2$	$C_{64}H_{82}N_4O_{18}Mg$
fw	915.48	1148.73	1271.82	1219.68
cryst size, mm	0.3 × 0.3 × 0.4	0.2 × 0.4 × 0.5	0.3 × 0.4 × 0.5	0.2 × 0.2 × 0.2
cryst syst	monoclinic	monoclinic	monoclinic	monoclinic
space group	$P2_1/c$	$P2_1/c$	$P2_1/n$	$P2_1/n$
a, Å	11.240(3)	16.611(5)	18.912(4)	15.210(5)
b, Å	13.019(2)	16.059(6)	16.254(2)	15.772(3)
c, Å	30.208(7)	21.930(9)	21.646(5)	13.093(3)
β, deg	99.11(1)	93.34(6)	112.26(2)	96.35(3)
V, Å^3	4365(2)	5840(4)	6158(2)	3122(1)
Z	4	4	4	2
T, °C	−71	−83	−74	−110
D_{calcd}, g cm^{-3}	1.39	1.31	1.37	1.30
abs coeff, cm^{-1}	1.30	1.46	1.69	1.03
transm factor	0.94−1.00	0.82−1.00	0.91−1.00	0.78−1.00
2θ range, deg	$3 < 2\theta < 50$	$3 < 2\theta < 45$	$3 < 2\theta < 46$	$3 < 2\theta < 45$
no. of unique data	8833	8317	8880	4254
no. of obsd data	5021 ($I > 3\sigma(I)$)	3759 ($I > 2\sigma(I)$)	5184 ($I > 3\sigma(I)$)	1840 ($I > 2\sigma(I)$)
no. of variables	560	613	785	278
R_{merge} (%)	3.0	3.0	2.6	7.8
R^a	0.045	0.069	0.060	0.069
$R_w{}^a$	0.054	0.085	0.072	0.070

[a] $R = \sum||F_o| - |F_c||/\sum|F_o|$; $R_w = [\sum w(|F_o| - |F_c|)^2/\sum w|F_o|^2]^{1/2}$, where $w = 1/\sigma^2(F_o)$. More details about the weighting scheme and other experimental protocols may be found in ref 27.

lent of bis(4-nitrophenyl) hydrogen phosphate (29.3 mg, 0.086 mmol) was added to a methanolic solution (2 mL) of **1**. The solution was stirred for 20−30 min and filtered through Celite. Vapor diffusion of ethyl ether into this solution afforded colorless, block crystals in 23% yield (24 mg, 0.020 mmol).

Method 2. A methanolic solution (2 mL) of $Mg(NO_3)_2$·$6H_2O$ (11 mg, 0.043 mmol) was added to a solution of H_2XDK (50 mg, 0.086 mmol) and NaOH (172 μL, 0.5 M in MeOH) in methanol (3 mL). The off-white product precipitated out of solution. The compound was washed with ether and dried under vacuum. Yield: 50% (26 mg, 0.021 mmol). ^{1}H NMR 300 MHz (CD_2Cl_2): δ 1.08 (br), 1.26 (br), 1.49 (br), 1.93 (s), 2.02 (br), 2.81 (br), 6.86 (s), 7.15 (s), 19.02 (br). IR (Nujol): 3462 (br), 1731 (m), 1680 (s), 1642 (m) (XDK), 1509, 1311, 1246, 1199 (m), 1085, 1026, 954, 854, 757 cm^{-1}. Anal. Calcd for $C_{64}H_{82}O_{18}N_4Mg$: C, 63.03; H, 6.78; N, 4.59. Found: C, 62.68; H, 6.86; N, 4.63.

Preparation of [Ca_2(XDK){μ-η^2-$(PhO)_2PO_2$}{η^1-$(PhO)_2PO_2$}-$(CH_3OH)_3(H_2O)$]·CH_3OH, 6·CH_3OH. A methanolic solution (1 mL) of $Ca(NO_3)_2$·$4H_2O$ (41 mg, 0.172 mmol) was added to a solution of H_2XDK (50 mg, 0.0861 mmol) and NaOH (350 μL, 0.5 M in MeOH) in methanol (3 mL). The solution was stirred at room temperature for 10 min, and a methanolic solution of NaDPP (47 mg, 0.172 mmol) was added. This mixture was stirred for another 10 min, and the solvent was removed in vacuo. The white residue was redissolved in methanol, and vapor diffusion of ethyl ether into the resulting solution afforded colorless needles. The crystals were collected and treated with excess pyridine (3 mL) in chloroform (5 mL). The inorganic salt contaminants were removed by filtration, and the py/$CHCl_3$ filtrate containing the complex was placed under vacuum to remove the solvents. The dried sample was redissolved in methanol. Vapor diffusion of ethyl ether into the solution gave long colorless block crystals of **6**·CH_3OH in 32% yield (35 mg, 0.0269 mmol). ^{1}H NMR, 300 MHz (CD_3OD): δ 1.18 (s, 6 H), 1.18 (d, 4 H, J = 13.5 Hz), 1.25 (s, 12 H), 1.55 (d, 2 H, J = 13.2 Hz), 1.90 (s, 6 H), 2.09 (d, 2 H, J = 13.3 Hz), 2.83 (d, 4 H, J = 13.1 Hz), 7.03 (m, 4 H), 7.13−7.26 (m, 17 H), 7.47 (s, 1 H). ^{31}P{^{1}H} NMR, 121.4 MHz (CD_3OD): δ −11.66 (s). IR (KBr): 3485 (br), 3053 (m), 2960 (s), 2918 (s), 2882 (s), 2429 (m), 1784, 1722 (s), 1682 (s), 1603 (s), 1489, 1452, 1414, 1366, 1203 (m, P−O), 1097 (s), 1025 (m), 916 (s), 834, 772, 689, 644, 518, 448 cm^{-1}. Anal. Calcd for $C_{60}H_{78}N_2O_{22}Ca_2P_2$ (**6**·CH_3OH·H_2O): C, 54.54; H, 5.95; N, 2.12. Found: C, 54.26; H, 5.55; N, 2.23.

X-ray Diffraction Studies of [Mg_2(XDK)$(CH_3OH)_4(H_2O)_2(NO_3)$]-(NO_3), 1(NO_3), [Mg_2(XDK){μ-η^2-$(PhO)_2PO_2$}$(CH_3OH)_3(H_2O)$-(NO_3)]·3CH_3OH, 2·3CH_3OH, [Mg_2(XDK){μ-η^2-$(PhO)_2PO_2$}{η^1-$(PhO)_2PO_2$}$(CH_3OH)_3(H_2O)$]·CH_3OH, 3·CH_3OH, and [Mg(HXDK)$_2$-$(H_2O)_2$], 4. Crystals of **1**(NO_3), **2**·3CH_3OH, **3**·CH_3OH, and **4** suitable for X-ray analyses were grown by ethyl ether diffusion into a methanolic solution of the complexes. Single-crystal X-ray diffraction experiments were carried out on an Enraf-Nonius CAD-4 diffractometer by using graphite-monochromated Mo Kα (λ = 0.710 69 Å) radiation. General procedures were previously described in detail.[27] The crystals were mounted at room temperature on the ends of quartz fibers in paratone and were judged to be of acceptable quality on the basis of open-counter ω-scans of several low-angle reflections and axial photographs. Crystallographic data are given in Table 1. All reflections were corrected for Lorentz−polarization effects, and an absorption correction was applied to the data for **3**·CH_3OH.

X-ray Diffraction Study of [Ca_2(XDK){μ-η^2-$(PhO)_2PO_2$}{η^1-$(PhO)_2PO_2$}$(CH_3OH)_3(H_2O)$]·CH_3OH, 6·CH_3OH. Crystals of **6**·CH_3OH were grown by diffusion of ethyl ether into a methanolic solution of the complex. Single-crystal X-ray diffraction studies of **6** were carried out on a Siemens CCD X-ray diffraction system controlled by a Pentium-based PC running the SMART version 4.0 software package,[28] as previously described.[29] A colorless block crystal of **6** was mounted at room temperature on the end of a glass fiber in paratone and data collection was carried out at −80 °C. The crystals were judged to be of acceptable quality on the basis of initial unit cell matrices and reflection profiles. Crystallographic data are given in Table 2.

Solution and Refinement of [Mg_2(XDK)$(CH_3OH)_4(H_2O)_2(NO_3)$]-(NO_3), 1(NO_3), [Mg_2(XDK){μ-η^2-$(PhO)_2PO_2$}$(CH_3OH)_3(H_2O)$-(NO_3)]·3CH_3OH, 2·3CH_3OH, [Mg_2(XDK){μ-η^2-$(PhO)_2PO_2$}{η^1-$(PhO)_2PO_2$}$(CH_3OH)_3(H_2O)$]·CH_3OH, 3·CH_3OH, and [Mg(HXDK)$_2$-$(H_2O)_2$], 4, Structures. All computations were carried out on DEC VAXstations. Calculations for **1**(NO_3) were performed with the TEXSAN crystallographic software package as described.[27] Calculations for **2**−**4** were made with an upgraded version of the TEXSAN software (Version 1.6).[30] Non-hydrogen atoms and the carboxylate hydrogen atom (H1) of **4** were located by direct methods and a series of least squares refinements. Carbon-bound hydrogen atoms for **1**−**3** were calculated at the ideal positions with a C−H distance of 0.95 Å. Non-hydrogen atoms for **1**−**3** were refined with anisotropic temperature factors. All carbon atoms in **4**, with the exception of the methyl

(27) Carnahan, E. M.; Rardin, R. L.; Bott, S. G.; Lippard, S. J. *Inorg. Chem.* **1992**, *31*, 5193−5201.
(28) SMART *Siemens Industrial Automation, Inc.*; Analytical Instrumentation: Madison, WI, 1994.
(29) Feig, A. L.; Bautista, M. T.; Lippard, S. J. *Inorg. Chem.* **1996**, *35*, 6892−6898.
(30) TEXSAN *Single Crystal Structure Analysis Software*; Molecular Structure Corporation: The Woodlands, TX, 1992.

Table 2. Crystallographic and Experimental Data for **6**·CH_3OH

formula	$C_{60}H_{76}N_2O_{21}Ca_2P_2$
fw	1303.33
cryst size, mm	0.3 × 0.3 × 0.5
cryst syst	monoclinic
space group	$P2_1/n$
a, Å	16.5471(3)
b, Å	24.3415(6)
c, Å	16.5865(3)
β, deg	104.2530(10)
V, Å^3	6475.1(2)
Z	4
T, °C	−80
D_{calcd}, g cm^{-3}	1.34
abs coeff, cm^{-1}	3.00
2θ range, deg	$3 < 2\theta < 46.53$
no. of unique data	9251
no. of obsd data ($I > 2\sigma(I)$)	7858
R_{merge} (%)	0.044
no. of variables	764
R^a	0.053
$wR^{2\,a}$	0.142

[a] $R = \sum||F_o| - |F_c||/\sum|F_o|$; $wR^2 = \{\sum[w(F_o^2 - F_c^2)^2]/\sum[w(F_o^2)^2]\}^{1/2}$, where $w = 1/\sigma^2(F_o)$. More details about the weighting scheme and other experimental protocols may be found in ref 29.

carbons and the carboxylate hydrogen atom (H1) were refined isotropically; non-carbon atoms and methyl carbons were refined anisotropically. Carbon-bound hydrogen atoms were not included in the final refinement.

Structure Solution and Refinement of [Ca_2(XDK){μ-η^2-(PhO)$_2$PO$_2$}{η^1-(PhO)$_2$PO$_2$}(CH$_3$OH)$_3$(H$_2$O)]·CH$_3$OH, 6·CH$_3$OH. Computations were carried out on Silicon Graphics Indy workstations. The raw data frames were processed by the SAINT version 4.0 software package.[31] All aspects of the structure solution and refinement were handled by the SHELXTL version 5.0 software package.[32] Non-hydrogen atoms were located by direct methods and a series of least-squares refinements and difference Fourier maps and were refined with anisotropic temperature factors.

Results and Discussion

Synthesis and Characterization of [Mg_2(XDK)(CH$_3$OH)$_4$(H$_2$O)$_2$(NO$_3$)](NO$_3$), 1(NO$_3$). The reaction of $Mg(NO_3)_2$·$6H_2O$ (2 equiv) with H_2XDK (1 equiv) and NaOH (2 equiv) in methanol and subsequent workup gave colorless crystals of [Mg_2(XDK)(CH$_3$OH)$_4$(H$_2$O)$_2$(NO$_3$)](NO$_3$), **1**(NO$_3$). The IR spectrum indicated the presence of the XDK ligand (1635−1714 cm^{-1}), nitrate anions (1301 cm^{-1}), and hydroxyl groups (∼ 3300−3400 cm^{-1}). The ^{1}H NMR spectrum in CD_3OD showed a symmetrical set of XDK resonances, with three singlets for the methyl groups of the ligand integrating at a ratio of 1:2:1 (δ 1.19, 1.29, and 1.93).

Crystals of **1**(NO$_3$) were obtained from a methanol/ethyl ether solvent system and chemical crystallographic analysis (CCA) revealed the features of a carboxylate-bridged, dinuclear magnesium(II) complex. The structure of the cation [Mg_2(XDK)(CH$_3$OH)$_4$(H$_2$O)$_2$(NO$_3$)]$^+$ (**1**) is given in Figure 2, and selected bond distances and angles are reported in Table 3. The magnesium(II) ions in **1** are 4.783(2) Å apart, separated by the two bridging carboxylates of the XDK^{2-} ligand. There are no other ligands bridging the two metal ions. The magnesium(II) ions and the carboxylate oxygen atoms are approximately coplanar, as indicated by the values of d, the distance of the Mg atoms from the dicarboxylate plane, and ϕ, the dihedral angle between [Mg1−Mg2−(O_{CO2})$_2$] and the carboxylate planes

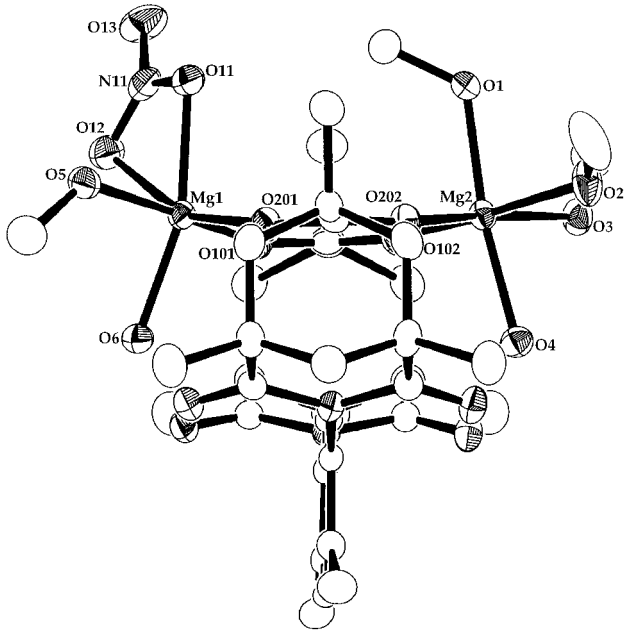

Figure 2. ORTEP view of [Mg_2(XDK)(CH$_3$OH)$_4$(H$_2$O)$_2$(NO$_3$)]$^+$ (**1**). Thermal ellipsoids are drawn at the 50% probability level, and hydrogen atoms are omitted for clarity.

Table 3. Selected Bond Distances (Å) and Angles (deg) for **1**(NO$_3$)[a]

Bond Distances			
Mg1−O5	2.098(3)	Mg2−O1	2.069(3)
Mg1−O6	2.056(2)	Mg2−O2	2.119(3)
Mg1−O11	2.144(3)	Mg2−O3	2.113(2)
Mg1−O12	2.242(3)	Mg2−O4	2.065(2)
Mg1−O101	2.003(2)	Mg2−O102	2.013(2)
Mg1−O201	1.956(2)	Mg2−O202	2.027(2)

Bond Angles			
O5−Mg1−O6	88.24(9)	O3−Mg2−O202	171.5(1)
O5−Mg1−O11	84.15(9)	O4−Mg2−O102	93.8(1)
O5−Mg1−O12	89.0(1)	O4−Mg2−O202	91.8(1)
O5−Mg1−O101	169.3(1)	O102−Mg2−O202	98.7(1)
O5−Mg1−O201	92.7(1)	Mg2−O1−C1	122.9(2)
O6−Mg1−O11	161.2(1)	Mg2−O2−C2	130.7(2)
O6−Mg1−O12	103.96(9)	Mg2−O3−C3	128.8(2)
O6−Mg1−O101	90.74(9)	Mg1−O5−C4	131.6(2)
O6−Mg1−O201	98.7(1)	Mg1−O11−N11	93.6(2)
O11−Mg1−O12	58.84(9)	Mg1−O12−N11	90.3(2)
O11−Mg1−O101	93.56(9)	Mg1−O101−C101	152.1(2)
O11−Mg1−O201	98.84(9)	Mg2−O102−C101	159.8(2)
O12−Mg1−O101	80.89(9)	Mg1−O201−C201	161.2(2)
O12−Mg1−O201	157.3(1)	Mg2−O202−C201	151.8(2)
O101−Mg1−O201	98.0(1)	O2−Mg2−O3	82.4(1)
O1−Mg2−O2	86.0(1)	O2−Mg2−O4	88.7(1)
O1−Mg2−O3	91.4(1)	O2−Mg2−O102	170.0(1)
O1−Mg2−O4	172.6(1)	O2−Mg2−O202	90.9(1)
O1−Mg2−O102	90.6(1)	O3−Mg2−O4	82.82(9)
O1−Mg2−O202	93.4(1)	O3−Mg2−O102	88.3(1)

[a] Estimated standard deviations are given in parentheses. See Figure 2 for atom labels.

(Table 4).[16,33] The metal ions are coordinated to the syn lone pairs of the carboxylates, with Mg−$OC_{carboxylate}$ bond angles ranging from 151.8(2) to 161.2(2)°.[33] Mg1 adopts a distorted octahedral geometry and is bound by one bidentate nitrate group (O11, O12), one methanol (O5), and one water molecule (O6). The geometric distortion is a consequence of the bidentate nitrate group, which coordinates unsymmetrically with relatively long Mg−O bonds (Table 3). The chelate ring of the nitrate anion

(31) SAINT *Siemens Industrial Automation, Inc.*; Analytical Instrumentation: Madison, WI, 1995.
(32) Sheldrick, G. M. *Siemens Industrial Automation, Inc.*; Analytical Instrumentation: Madison, WI, 1994.
(33) Carrell, C. J.; Carrell, H. L.; Erlebacher, J.; Glusker, J. P. *J. Am. Chem. Soc.* **1988**, *110*, 8651−8656.

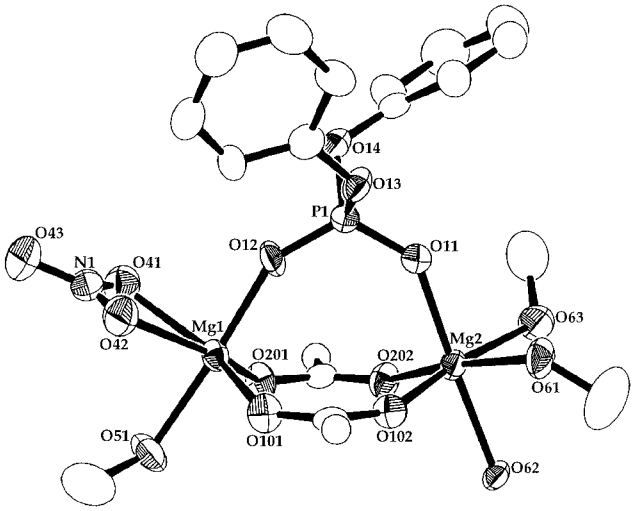

Figure 3. ORTEP plot of the dinuclear center of $[Mg_2(XDK)\{\mu\text{-}\eta^2\text{-}(PhO)_2PO_2\}(CH_3OH)_3(H_2O)(NO_3)]$ (**2**). Hydrogen atoms and all atoms of the XDK ligand, except the carboxylate groups, are omitted for clarity.

is approximately perpendicular to the [Mg1−O101−O201] plane (dihedral angle, 94°). The Mg1 bond distances to the XDK^{2-} carboxylates are shorter than the average $Mg-O_{carboxylate}$ bond distance of 2.04 Å[33] (Table 3). Mg2 is octahedrally coordinated by three methanol ligands (O1, O2, and O3) and one water molecule (O4) in addition to the bridging carboxylates from the XDK^{2-} ligand (O102, O202). The Mg2 bond distances to the carboxylate oxygens are slightly longer than those of Mg1. The water molecules on both metal ions (O4 and O6) are each hydrogen bonded to the imide carbonyl oxygens on the XDK ligand. The oxygen−oxygen hydrogen-bonded distances from O4 to O104 and O203 are 2.83 and 2.78 Å, respectively, and the distances from O6 to O103 and O204 are 2.78 and 2.80 Å, respectively (Figures 2 and S1).

Although the crystal structure of **1** reveals the two magnesium(II) ions to be in different environments, the ^1H NMR spectrum of this compound in CD_3OD indicates that the metal ions are equivalent in solution. This result suggests either that the coordinated nitrate anion is displaced by methanol in solution or that it exchanges rapidly on the NMR time scale.

Synthesis and Characterization of $[Mg_2(XDK)\{\mu\text{-}\eta^2\text{-}(PhO)_2PO_2\}(CH_3OH)_3(H_2O)(NO_3)]\cdot 3CH_3OH$, $2\cdot 3CH_3OH$. Addition of NaDPP (1 equiv) to a methanolic solution of **1** (1 equiv) gave the desired diphenyl phosphate-bridged product as the methanol solvate, $[Mg_2(XDK)\{\mu\text{-}\eta^2\text{-}(PhO)_2PO_2\}(CH_3OH)_3(H_2O)(NO_3)]\cdot 3CH_3OH$, ($\mathbf{2}\cdot 3CH_3OH$). The IR spectrum of **2** revealed the presence of XDK, nitrate, diphenyl phosphate (1231 cm^{-1}), and hydroxyl groups. The ^1H NMR spectrum of **2** in CD_3OD suggested C_{2v} symmetry for the XDK ligand, as exemplified by the three singlets observed for the methyl groups of the ligand in a 1:2:1 intensity ratio (δ 1.23, 1.26, and 1.90). The proton NMR spectrum also showed multiplets in the aromatic region (∼7.0−7.2 ppm) corresponding to the phenyl groups of diphenyl phosphate. The $^{31}P\{^1H\}$ NMR spectrum of **2** in CD_3OD at room temperature suggested the presence of a coordinated diphenyl phosphate ligand with a resonance at −15.46 ppm, which is 6.32 ppm upfield from that of free diphenyl phosphate.

Crystals of $\mathbf{2}\cdot 3CH_3OH$ were grown by vapor diffusion of ethyl ether into a methanolic solution of **2**. An X-ray diffraction study confirmed the structure to contain a dinuclear magnesium(II) XDK complex with a bidentate bridging diphenyl phosphate ligand. The structure of the complex is depicted in Figure 3, and selected bond distances and angles are given in Table 5. The magnesium(II) ions in **2** are situated 4.240(5) Å apart. They are coordinated to the syn lone pairs of the carboxylates and displaced from the plane of the carboxylate oxygens by 0.75 and 0.55 Å, for Mg1 and Mg2, respectively (Table 4). The dihedral angle of 3.0° between the planes of the two carboxylate groups indicates that they are approximately coplanar. Mg1 has a distorted octahedral geometry similar to that of Mg1 in compound **1**, with one methanol (O51), one bidentate nitrate group (O41, O42), XDK^{2-} carboxylate oxygen atoms (O101, O201), and a phosphate ester oxygen atom (O12). The bidentate nitrate ligand is coordinated unsymmetrically to Mg1 (Table 5) and is approximately perpendicular to the magnesium(II)-phosphinyl, [Mg1−O12−P1−O11−Mg2], plane (94°) and roughly parallel to the [Mg1−O101−O201] plane (15°). Mg2 is octahedrally coordinated by two methanol ligands (O61 and O63), one water molecule (O62), XDK^{2-} carboxylate oxygen atoms (O102, O202), and a phosphate ester oxygen atom (O11). The O11−P1−O12 angle has been increased from the usual tetrahedral value to 121.2(4)°, whereas the other angles around the phosphorus atom only deviate slightly from tetrahedral. The distortion around the phosphinyl center appears to derive from the bridging bidentate coordination mode to the two magnesium atoms. The O11−P1−O12 bond angle is similar to those found in other dimetallic complexes containing $\mu\text{-}\eta^2$ phosphate ester ligands.[22,24,34−40] The P1−O11 and P1−O12 bond distances are significantly shorter than the P1−O13 and P1−O14 distances (Table 5). Such differences in the $P-O_{metal}$ vs $P-O_C$ bond distances are common.[22,24,34−43]

The diphenyl phosphate ligand is coordinated to the magnesium atoms through its syn lone pairs, which is the typical coordination mode for phosphate−metal ion interactions.[44] The P1−O12−Mg1 and P1−O11−Mg2 bond angles of 141.1(4) and 138.8(4)°, respectively, are comparable to those observed in other phosphorus−oxygen−metal bond angles (141°, average value).[44] The magnesium(II) ions are approximately coplanar with the phosphinyl group, as indicated by the dihedral angle of 4° between the [P1−O11−O12] and [Mg1−Mg2−O11−O12] planes and the displacement of Mg1 and Mg2 from the [P1−O11−O12] plane (0.04 and 0.20 Å, respectively). This "in-plane" coordination mode for the magnesium atoms to phosphate is less common than the 0.9 Å "out-of-plane" location reported for other phosphate-metal ion compounds.[44] The magnesium−phosphinyl plane is perpendicular to the plane of the xylyl ring (dihedral angle, 90°).

(34) Armstrong, W. H.; Lippard, S. J. *J. Am. Chem. Soc.* **1985**, *107*, 3730−3731.
(35) Turowski, P. N.; Armstrong, W. H.; Roth, M. E.; Lippard, S. J. *J. Am. Chem. Soc.* **1990**, *112*, 681−690.
(36) Turowski, P. N.; Armstrong, W. H.; Liu, S.; Brown, S. N.; Lippard, S. J. *Inorg. Chem.* **1994**, *33*, 636−645.
(37) Krebs, B.; Schepers, K.; Bremer, B.; Henkel, G.; Althaus, E.; Muller-Warmuth, W.; Griesar, K.; Haase, W. *Inorg. Chem.* **1994**, *33*, 1907−1914.
(38) Jang, H. G.; Hendrich, M. P.; Que, L., Jr. *Inorg. Chem.* **1993**, *32*, 911−918.
(39) Mahroof-Tahir, M.; Karlin, K. D.; Chen, Q.; Zubieta, J. *Inorg. Chim. Acta* **1993**, *207*, 135−138.
(40) Hikichi, S.; Tanaka, M.; Moro-oka, Y.; Kitajima, N. *J. Chem. Soc., Chem. Commun.* **1992**, 814−815.
(41) Drueke, S.; Wieghardt, K.; Nuber, B.; Weiss, J.; Fleischhauser, H.-P.; Gehring, S.; Haase, W. *J. Am. Chem. Soc.* **1989**, *111*, 8622−8631.
(42) Norman, R. E.; Yan, S.; Que, L., Jr.; Backes, G.; Ling, J.; Sanders-Loehr, J.; Zhang, J. H.; O'Connor, C. J. *J. Am. Chem. Soc.* **1990**, *112*, 1554−1562.
(43) Schepers, K.; Bremer, B.; Krebs, B.; Henkel, G.; Althaus, E.; Mosel, B.; Muller-Warmuth, W. *Angew. Chem., Int. Ed. Engl.* **1990**, *29*, 531−533.
(44) Alexander, R. S.; Kanyo, Z. F.; Chirlian, L. E.; Christianson, D. W. *J. Am. Chem. Soc.* **1990**, *112*, 933−937.

Table 4. Structural Parameters of **1**(NO_3), **2**·3CH_3OH, **3**·CH_3OH, **5**, and **6**·CH_3OH

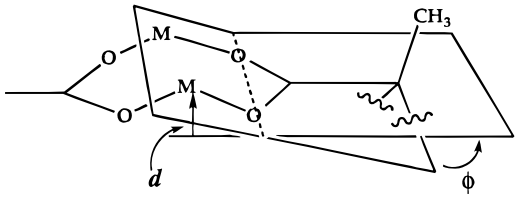

	1(NO_3)	**2**·3CH_3OH	**3**·CH_3OH	**5**[e]	**6**·CH_3OH
M1···M2, Å	4.783(2)	4.240(5)	4.108(3)	3.869(2)	4.4628(9)
M1−O(XDK)$_{av}$, Å[a]	1.980(3)	1.975(10)	1.983(6)	1.938(6)	2.335(3)
M2−O(XDK)$_{av}$, Å[a]	2.020(3)	2.040(10)	2.059(6)	2.084(7)	2.269(3)
O101−M1−O201, deg	98.0(1)	110.5(3)	122.2(2)	127.6(2)	113.83(9)
O102−M2−O202, deg	98.7(1)	101.0(3)	100.3(2)	96.6(2)	94.76(9)
O11−P1−O12, deg		121.2(4)	118.9(3)	118.8(3)	118.5(2)
P1−O12−M1, deg		149.1(4)	141.9(3)	137.6(3)	151.1(2)
P1−O11−M2, deg		138.8(4)	138.4(3)	135.8(3)	139.1(2)
ϕ, deg[b]	9.8	22.7	19.4	21.7	23.7
d(M1), Å[c]	0.31	0.75	0.50	0.70	0.87
d(M2), Å[c]	0.21	0.55	0.71	0.61	0.71
[O(101)O(102)C(101)C(107)] vs [O(201)O(202)C(201)C(207)], deg[d]	6.5	3.0	8.3	11	6.1

[a] Average value. Estimated deviations in parentheses are derived from $(\sigma_A^2 + \sigma_B^2)^{1/2}$. [b] Dihedral angle between the [M1M2(O_{CO2})$_2$] and the dicarboxylate planes (average value). [c] Distance from the metal atom to the dicarboxylate plane. [d] Dihedral angle. [e] Reference 24.

Table 5. Selected Bond Distances (Å) and Angles (deg) for **2**·3CH_3OH[a]

Bond Distances			
Mg1−O12	2.003(7)	Mg1−O101	1.973(7)
Mg1−O41	2.237(8)	Mg1−O201	1.976(7)
Mg1−O42	2.164(8)	Mg2−O11	2.003(7)
Mg1−O51	2.118(8)	Mg2−O61	2.131(7)
P1−O11	1.481(7)	Mg2−O62	2.125(7)
P1−O12	1.467(6)	Mg2−O63	2.121(8)
P1−O13	1.601(7)	Mg2−O102	2.040(7)
P1−O14	1.587(7)	Mg2−O202	2.039(7)
Bond Angles			
O11−P1−O12	121.2(4)	O61−Mg2−O62	86.4(3)
O11−P1−O13	104.0(4)	O61−Mg2−O63	85.3(3)
O11−P1−O14	110.9(4)	O61−Mg2−O102	85.2(3)
O12−P1−O13	110.6(4)	O61−Mg2−O202	170.1(3)
O12−P1−O14	105.3(4)	O62−Mg2−O63	87.4(3)
O13−P1−O14	103.5(4)	O62−Mg2−O102	88.4(3)
O12−Mg1−O41	89.0(3)	O62−Mg2−O202	86.1(3)
O12−Mg1−O42	91.5(3)	O63−Mg2−O102	169.9(3)
O12−Mg1−O51	176.3(3)	O63−Mg2−O202	87.9(3)
O12−Mg1−O101	94.6(3)	O102−Mg2−O202	101.0(3)
O12−Mg1−O201	98.4(3)	P1−O11−Mg2	138.8(4)
O41−Mg1−O42	58.2(3)	P1−O12−Mg1	149.1(4)
O41−Mg1−O51	87.3(3)	P1−O13−C7	126.9(6)
O41−Mg1−O101	153.9(3)	P1−O14−C1	124.8(6)
O41−Mg1−O201	94.4(3)	Mg1−O41−N41	91.6(7)
O42−Mg1−O51	86.0(3)	Mg1−O42−N41	93.8(7)
O42−Mg1−O101	95.9(3)	Mg1−O51−C51	128.9(7)
O42−Mg1−O201	150.8(3)	Mg2−O61−C61	130.2(7)
O51−Mg1−O101	88.5(3)	Mg2−O63−C63	125.4(7)
O51−Mg1−O201	82.5(3)	Mg1−O101−C101	136.3(7)
O101−Mg1−O201	110.5(3)	Mg2−O102−C101	153.2(6)
O11−Mg2−O61	93.0(3)	Mg1−O201−C201	140.6(6)
O11−Mg2−O62	178.2(3)	Mg2−O202−C201	150.2(7)
O11−Mg2−O63	90.9(3)	O11−Mg2−O102	93.2(3)
O11−Mg2−O202	94.3(3)		

[a] Estimated standard deviations are given in parentheses. See Figure 3 for atom labels.

Synthesis and Characterization of [Mg_2(XDK){μ-η^2-$(PhO)_2PO_2$}{η^1-$(PhO)_2PO_2$}$(CH_3OH)_3(H_2O)$]·CH_3OH, 3·CH_3OH. Addition of 2 equiv of NaDPP to a methanol solution containing **1** gave [Mg_2(XDK){μ-η^2-$(PhO)_2PO_2$}{η^1-$(PhO)_2PO_2$}$(CH_3OH)_3(H_2O)$]·CH_3OH, (**3**·CH_3OH). The IR spectrum of **3** indicated the presence of XDK, diphenyl phosphate, and hydroxyl groups. The ^{1}H NMR spectrum of **3** in CD_3OD showed three singlets for the methyl groups of XDK (δ 1.23, 1.26, and 1.90) integrating at a 1:2:1 ratio, suggesting a symmetrical C_{2v} environment for the ligand. The phenyl protons of diphenyl phosphate appeared as multiplet signals in the aromatic region (∼7.0−7.2 ppm), integration of which revealed a DPP:XDK ratio of 2:1. The ^{31}P{^{1}H} NMR spectrum of **3** in CD_3OD at room temperature contained 2 signals at −9.14 and −15.45 ppm, corresponding to free and bound diphenyl phosphate, respectively. This assignment was made by using the ^{31}P{^{1}H} NMR spectrum of **2** (δ −15.46) for the bound phosphate ester. Addition of 1 equiv of (Me_4N)DPP to a sample of **3** gave a ^{31}P{^{1}H} NMR spectrum which integrated for a 2:1 ratio of free-to-bound phosphodiester groups. These results indicate that the bridging phosphate ester ligand is more stable to dissociation than the terminal one. Although the ^{31}P{^{1}H} NMR signal of terminally bound diphenyl phosphate may be the same as that of free DPP^-, conductivity measurements of **3** in methanol revealed it to be a 1:1 electrolyte, consistent with the observation of a dissociated diphenyl phosphate ligand.

Crystals of **3**·CH_3OH were grown from a methanol/ethyl ether solvent system, and CCA revealed its structure to consist of a dinuclear magnesium(II) center bridged by the carboxylate oxygens of the XDK ligand and one bidentate diphenyl phosphate. The structure of [Mg_2(XDK){μ-η^2-$(PhO)_2PO_2$}{η^1-$(PhO)_2PO_2$}$(CH_3OH)_3(H_2O)$] is shown in Figure 4, and selected bond distances and angles are given in Table 6. Mg1 is additionally coordinated by a terminal, monodentate DPP ligand (O21) and a water molecule (O51), which afford trigonal bipyramidal geometry. Mg2 has three methanol ligands (O61, O62, and O63) to complete its octahedral coordination sphere. The shorter average Mg1−O bond length of 2.015Å compared to the average Mg2−O distance of 2.073Å is consistent with the lower coordination number of Mg1. The magnesium atoms are displaced from the plane of the carboxylates (d = 0.50 and 0.71 Å, for Mg1 and Mg2 respectively), with a Mg···Mg separation of 4.108(3) Å.

The O11−P1−O12 angle in the bidentate, bridging diphenyl phosphate ligand in **3** is 118.9(3)°, whereas the other angles only deviate slightly from tetrahedral values (Table 6). An exception is the O13−P1−O14 angle, which is 97.4(2)°. The P1−O11 and P1−O12 bond lengths are significantly shorter

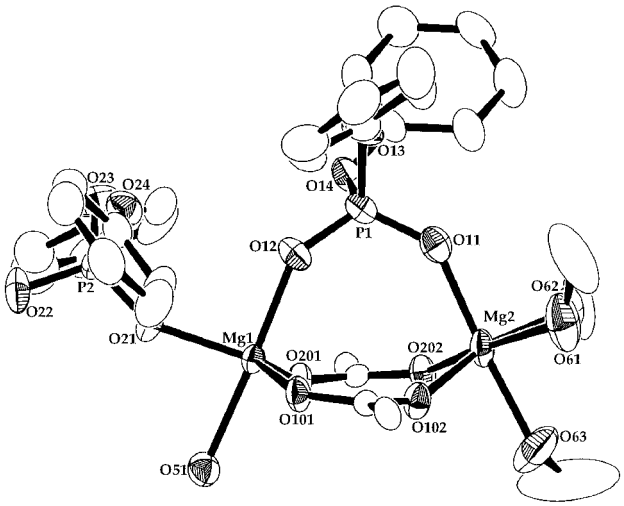

Figure 4. ORTEP diagram of the dinuclear core of $[Mg_2(XDK)\{\mu\text{-}\eta^2\text{-}(PhO)_2PO_2\}\{\eta^1\text{-}(PhO)_2PO_2\}(CH_3OH)_3(H_2O)]$ (**3**). Hydrogen atoms and all atoms of the XDK ligand, except the carboxylate groups, are omitted for clarity.

Table 6. Selected Bond Distances (Å) and Angles (deg) for **3**·CH_3OH[a]

	Bond Distances		
Mg1−O12	2.015(4)	Mg2−O11	2.018(5)
Mg1−O21	1.949(4)	Mg2−O61	2.153(6)
Mg1−O51	2.145(5)	Mg2−O62	2.125(5)
Mg1−O101	1.986(4)	Mg2−O63	2.024(6)
Mg1−O201	1.979(4)	Mg2−O102	2.052(5)
P1−O11	1.472(4)	Mg2−O202	2.065(4)
P1−O12	1.470(4)	P2−O21	1.481(4)
P1−O13	1.599(4)	P2−O22	1.473(4)
P1−O14	1.586(4)	P2−O23	1.583(5)
		P2−O24	1.598(5)
	Bond Angles		
O11−P1−O12	118.9(3)	O11−Mg2−O202	95.0(2)
O11−P1−O13	109.1(2)	O61−Mg2−O62	81.7(2)
O11−P1−O14	112.0(2)	O61−Mg2−O63	84.2(3)
O12−P1−O13	111.9(3)	O61−Mg2−O102	89.0(2)
O12−P1−O14	105.4(2)	O61−Mg2−O202	169.1(2)
O13−P1−O14	97.4(2)	O62−Mg2−O63	86.8(2)
O21−P2−O22	115.8(3)	O62−Mg2−O102	166.8(2)
O21−P2−O23	109.9(3)	O62−Mg2−O202	88.1(2)
O21−P2−O24	111.3(2)	O63−Mg2−O102	82.8(2)
O22−P2−O23	112.8(3)	O63−Mg2−O202	91.5(3)
O22−P2−O24	110.2(3)	O102−Mg2−O202	100.3(2)
O23−P2−O24	95.1(2)	P1−O11−Mg2	138.4(3)
O12−Mg1−O21	92.6(2)	P1−O12−Mg1	141.9(3)
O12−Mg1−O51	176.5(2)	P1−O13−C11	123.7(4)
O12−Mg1−O101	93.7(2)	P1−O14−C21	127.2(4)
O12−Mg1−O201	95.6(2)	P2−O21−Mg1	151.7(3)
O21−Mg1−O51	84.8(2)	P2−O23−C31	121.2(4)
O21−Mg1−O101	112.5(2)	P2−O24−C41	119.8(4)
O21−Mg1−O201	123.9(2)	Mg2−O61−C61	132.7(6)
O51−Mg1−O101	85.1(2)	Mg2−O62−C62	132.6(4)
O51−Mg1−O201	87.8(2)	Mg2−O63−C63	129.8(8)
O101−Mg1−O201	122.2(2)	Mg1−O101−C101	127.7(4)
O11−Mg2−O61	89.5(2)	Mg2−O102−C101	153.9(4)
O11−Mg2−O62	93.6(2)	Mg1−O201−C201	146.0(4)
O11−Mg2−O63	173.6(3)	Mg2−O202−C201	141.8(4)
O11−Mg2−O102	95.8(2)		

[a] Estimated standard deviations are given in parentheses. See Figure 4 for atom labels.

than the P1−O13 and P1−O14 distances (Table 6), similar to those observed in **2**. The bridging diphenyl phosphate ligand coordinates to the magnesium atoms in a syn−syn manner, as indicated by the P1−O12−Mg1 and P1−O11−Mg2 bond angles (Table 4). The [Mg1−O12−P1−O11−Mg2] plane is approximately perpendicular to plane of the xylyl ring (96°).

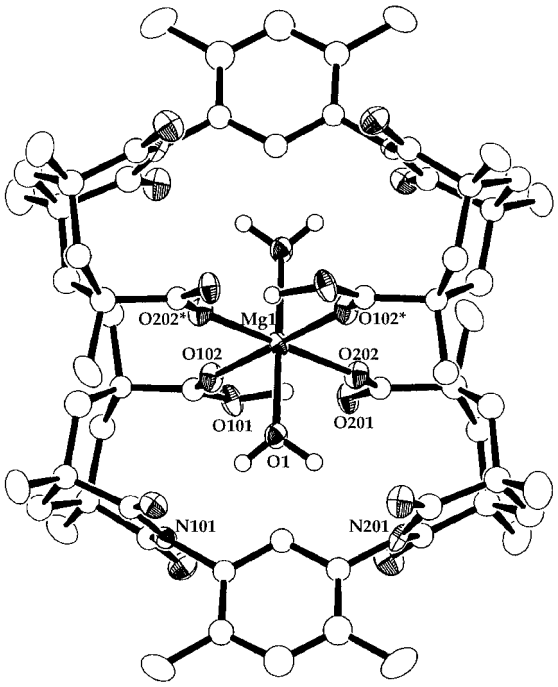

Figure 5. ORTEP view of $[Mg(HXDK)_2(H_2O)_2]$ (**4**). Thermal ellipsoids are drawn at the 50% probability level, and some hydrogen atoms are omitted for clarity.

Mg1 and Mg2 have been displaced from the [P1−O11−O12] plane by 0.74 and 0.70 Å, respectively, which is similar to that observed for other phosphate−metal complexes.[44]

In the monodentate, terminal diphenyl phosphate ligand, the phosphorus atom is roughly tetrahedral, with only one deviating angle (O21−P2−O22 = 115.8(3)°). The P2−O21 bond length of 1.481(4) Å is only slightly longer than the P2−O22 bond length of 1.473(4) Å. The P2−O23 and P2−O24 bond lengths are 1.583(5) and 1.598(5) Å, respectively. There are relatively few dimetallic complexes containing a terminally coordinated phosphate ligand.[22,24,45−47]

Synthesis and Characterization of $[Mg(HXDK)_2(H_2O)_2]$, 4. Addition of one equiv of bis(4-nitrophenyl) hydrogen phosphate (HBNPP) to a methanolic solution of **1** gave $[Mg(HXDK)_2(H_2O)_2]$ (**4**), the IR spectrum of which indicated the presence of XDK and hydroxyl groups. The ^1H NMR spectrum of **4** in CD_2Cl_2 showed some broad features which corresponded to the XDK ligand and a signal at 19.0 ppm consistent with that of a carboxylate proton and characteristic of a short, low-barrier hydrogen bond.[48]

Crystals of **4** were grown by vapor diffusion of ethyl ether into a methanol solution containing **4**. The X-ray crystal structure of **4** revealed a mononuclear magnesium(II) center coordinated by two HXDK ligands. The structure of $[Mg(HXDK)_2(H_2O)_2]$ (**4**) is presented in Figure 5. Selected bond distances and angles are given in Table 7. The magnesium(II) ion sits on an inversion center and is octahedrally coordinated by the HXDK carboxylate ligands and two water molecules. The magnesium atom is displaced by 0.38 Å from the dicar-

(45) Bremer, B.; Schepers, K.; Fleischhauer, P.; Haase, W.; Henkel, G.; Krebs, B. *J. Chem. Soc., Chem. Commun.* **1991**, 510−512.
(46) Glowiak, T.; Podgorska, I.; Baranowski, J. *Inorg. Chim. Acta* **1986**, *115*, 1−10.
(47) Sarneksi, J. E.; Didiuk, M.; Thorp, H. H.; Crabtree, R. H.; Brudvig, G. W.; Faller, J. W.; Schulte, G. K. *Inorg. Chem.* **1991**, *30*, 2833−2835.
(48) (a) Cleland, W. W.; Kreevoy, M. M. *Science* **1994**, *264*, 1887−1890. (b) Kato, Y.; Toledo, L. M.; Rebek, J., Jr. *J. Am. Chem. Soc.* **1996**, *118*, 8575−8579.

Table 7. Selected Bond Distances (Å) and Angles (deg) for **4**[a]

Bond Distances			
Mg1−O1	2.090(6)	Mg1−O202	2.084(5)
Mg1−O102	2.043(5)	O101−O201	2.423(8)
Bond Angles			
O1−Mg1−O102	86.6(2)	O102−Mg1−O202	94.4(2)
O1−Mg1−O102*	93.4(2)	O102−Mg1−O202*	85.6(2)
O1−Mg1−O202	88.3(2)	Mg1−O102−C101	151.2(6)
O1−Mg1−O202*	91.7(2)	Mg1−O202−C201	149.3(6)

[a] Estimated standard deviations are given in parentheses. See Figure 5 for atom labels.

boxylate plane. The two carboxylate groups are approximately coplanar, with a dihedral angle of 4.7° between them. The distance between O101 and O201 is 2.423(8) Å.

The magnesium(II) ions in **1** dissociate from XDK under acidic conditions as evidenced by the formation of **4**. Protonation of one of the XDK carboxylates under acidic conditions is not unexpected since its pK_a value is unusually high (pK_a = 11.1 in 1:1 EtOH/H_2O).[49]

Synthesis and Characterization of [Ca_2(XDK){μ-η^2-(PhO)$_2$PO$_2$}{η^1-(PhO)$_2$PO$_2$}(CH$_3$OH)$_3$(H_2O)]·CH$_3$OH, 6·CH$_3$OH. Reaction of $Ca(NO_3)_2$·4H_2O (2 equiv) with H_2XDK (1 equiv) and NaOH (2 equiv) in methanol, followed by the addition of NaDPP (2 equiv), gave the desired dicalcium(II) analog [Ca_2(XDK){μ-η^2-(PhO)$_2$PO$_2$}{η^1-(PhO)$_2$PO$_2$}(CH$_3$OH)$_3$(H_2O)]·CH$_3$OH, (**6**·CH$_3$OH). The IR spectrum indicated the presence of XDK, diphenyl phosphate, and hydroxyl groups. The ^{1}H NMR spectrum in CD_3OD showed singlets for the methyl groups of XDK (δ 1.18, 1.25, and 1.90) and doublets for the methylene groups (δ 1.18, 1.55, 2.09, and 2.83), consistent with C_{2v} symmetry. The phenyl protons of diphenyl phosphate gave multiplet signals in the aromatic region, and integrations showed a DPP:XDK ratio of 2:1. The ^{31}P NMR spectrum of **6** in CD_3OD at room temperature exhibited one sharp singlet at −11.66 ppm. Conductivity measurements of **6** in methanol revealed it to be a 1:1 electrolyte, indicating dissociation of a diphenyl phosphate in solution.

X-ray quality crystals of **6** were grown from a methanol/ethyl ether solvent system, and CCA revealed a polymeric structure in the solid state. The repeating unit comprises a dinuclear calcium(II) center bridged by the carboxylates of XDK and by a bidentate diphenyl phosphate ligand (Figure 6). Selected bond distances and angles are given in Table 8. We hereafter refer to this unit as the intramolecularly-bridged dicalcium(II) moiety. The structure of **6** differs slightly from that of the dimagnesium(II) (**3**) and the dizinc(II) (**5**) analogs since both calcium(II) ions are octahedrally coordinated. The other diphenyl phosphate ligand coordinates to one calcium atom (Ca1) and forms a bridge to the calcium (Ca2A) of a neighboring unit, generating the polymer (Figure 7). The Ca1 and Ca2 atoms are displaced by 0.87 and 0.71 Å, respectively, from the dicarboxylate plane (Table 4). Ca1 is octahedrally coordinated by the bridging phosphates (O12) and (O21), the carboxylates of XDK (O101 and O201), and two methanol ligands (O51 and O52). The Ca1−O101 and Ca1−O201 bond distances are similar to the reported average Ca−$O_{carboxylate}$ bond distance of 2.3 Å for a coordination number of 6.[33] Ca2 is also octahedrally coordinated by the bridging phosphate (O11), the other phosphate of a neighboring molecule (O22A), the carboxylate oxygens of XDK (O102 and O202), a methanol (O62), and a water molecule (O61). The Ca2 bond distances to O102 and O202 are slightly shorter than those of Ca1. The calcium atoms

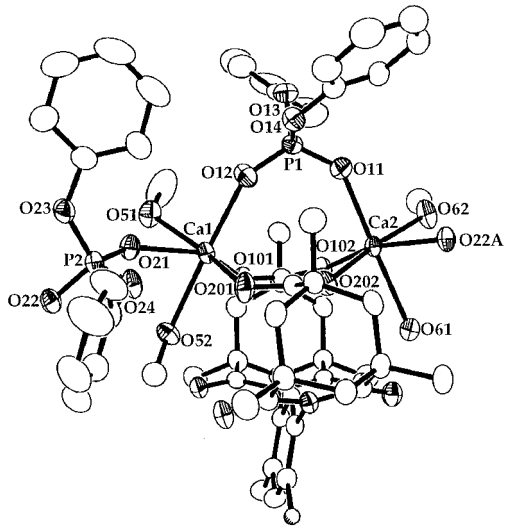

Figure 6. ORTEP diagram of [Ca_2(XDK){μ-η^2-(PhO)$_2$PO$_2$}{η^1-(PhO)$_2$PO$_2$}(CH$_3$OH)$_3$(H_2O)], (**6**). Thermal ellipsoids are drawn at the 50% probability level. Hydrogen atoms are omitted for clarity.

Table 8. Selected Bond Distances (Å) and Angles (deg) for **6**·CH$_3$OH[a]

Bond Distances			
Ca1−O12	2.295(3)	Ca2−O202	2.240(2)
Ca1−O21	2.306(2)	Ca2−O11	2.282(2)
Ca1−O201	2.318(2)	Ca2−O22A	2.289(2)
Ca1−O101	2.351(2)	Ca2−O102	2.298(2)
Ca1−O51	2.388(2)	Ca2−O62	2.394(2)
Ca1−O52	2.430(2)	Ca2−O61	2.457(2)
P1−O12	1.472(3)	P2−O22	1.475(2)
P1−O11	1.482(3)	P2−O21	1.477(2)
P1−O13	1.602(2)	P2−O24	1.594(2)
P1−O14	1.603(3)	P2−O23	1.600(3)
Bond Angles			
O12−Ca1−O21	104.31(9)	O202−Ca2−O11	91.41(9)
O12−Ca1−O201	91.31(10)	O202−Ca2−O22A	94.05(9)
O21−Ca1−O201	86.66(9)	O11−Ca2−O22A	96.31(9)
O12−Ca1−O101	101.57(9)	O202−Ca2−O102	94.76(9)
O21−Ca1−O101	146.45(9)	O11−Ca2−O102	100.55(9)
O201−Ca1−O101	113.83(9)	O22A−Ca2−O102	160.75(9)
O12−P1−O11	118.5(2)	O22−P2−O21	119.67(14)
O12−P1−O13	110.8(2)	O22−P2−O24	110.11(14)
O11−P1−O13	109.69(14)	O21−P2−O24	106.92(13)
O12−P1−O14	106.69(14)	O22−P2−O23	104.71(13)
O11−P1−O14	111.55(14)	O21−P2−O23	110.81(14)
O13−P1−O14	97.52(13)	O24−P2−O23	103.50(14)
P1−O11−Ca2	139.1(2)	P2−O21−Ca1	151.3(2)
P1−O12−Ca1	151.1(2)	P2−O22−Ca2A	139.27(14)

[a] Estimated standard deviations are given in parentheses. See Figure 6 for atom labels.

are coordinated to the syn lone pairs of the carboxylates, as suggested by the average Ca1− and Ca2−$OC_{carboxylate}$ bond angles of 132.6(3) and 153.4(3)°, respectively. This mode of calcium binding to carboxylate groups is often observed.[33] The Ca···Ca distance is 4.4628(9) Å, which is longer than the M···M distances in **3** and **5** (Table 4). The longer metal−metal separation in **6** may be due to the greater ionic radius of calcium(II)[50] and to the effect of the terminal diphenyl phosphate bridging the calcium(II) ions in two asymmetric units.

The O11−P1−O12 angle in **6** is slightly smaller than the O21−P2−O22 angle (Table 8). The phosphorus−oxygen bond distances are shorter to the metal-coordinated oxygens in both P1 and P2 (Table 8), which is similar to that observed for **3**. The calcium(II) ions are coordinated to the syn lone pairs of

(49) Rebek, J., Jr.; Duff, R. J.; Gordon, W. E.; Parris, K. *J. Am. Chem. Soc.* **1986**, *108*, 6068−6069.

(50) Shannon, R. B. *Acta Crystallogr.* **1976**, *32A*, 751−767.

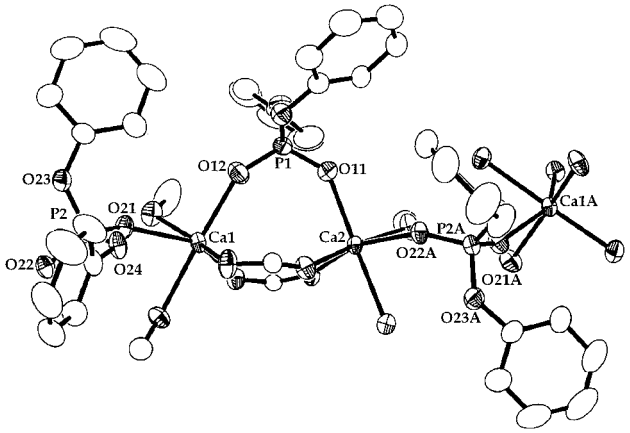

Figure 7. ORTEP view of the polymeric calcium center in **6**.

the bridging phosphate, as suggested by the Ca1− and Ca2−O−P1 bond angles (Table 4). The Ca1 and Ca2 atoms lie roughly in the plane defined by the phosphinyl group, [O11−P1−O12], as indicated by displacements of 0.27 and 0.37 Å for Ca1 and Ca2, respectively, and the 8° dihedral angle between the phosphinyl plane and the [Ca1−O12−P1−O11-Ca2] plane. The [Ca1−Ca2−O11−O12] plane is approximately perpendicular to that of the xylyl spacer (89°). Ca2 and Ca1A are displaced by −1.1 and +1.0 Å, respectively, from the [O21A−P2A−O22A] plane (Figure 7). Ca2 and Ca1A are coordinated to the syn lone pairs of the phosphate. The Ca1−O21−P2 and Ca2−O22A−P2A bond angles are 151.3(2) and 139.27(14)°. The P2A phosphinyl plane is 87° from the P1 phosphinyl plane.

Variable-Temperature $^{31}P\{^1H\}$ NMR Studies. Samples of **3**, **5**, and **6** (30 mM) in CD_3OD were studied by VT $^{31}P\{^1H\}$ NMR spectroscopy. Each compound exhibited two sharp singlets in its low-temperature limiting spectrum. Compound **3** displayed resonances at δ −9.07 and −15.69, corresponding to free and bound diphenyl phosphate, respectively. This assignment was made by addition of $(Me_4N)DPP$ to confirm the identity of the free diphenyl phosphate resonance and by comparison to the ^{31}P chemical shift of $[Mg_2(XDK)\{\mu\text{-}\eta^2\text{-}(PhO)_2PO_2\}(CH_3OH)_3(H_2O)(NO_3)]$ at δ −15.46. Complexation of magnesium(II), zinc(II), and calcium(II) ions to phosphate esters shifts the ^{31}P NMR signals to lower fields.[51] Figure 8 shows spectra of **3** over the temperature range $-24 \le T \le 60$ °C, indicating diphenyl phosphate exchange at elevated temperatures. The free energy of activation for phosphate ester exchange was estimated from the coalescence temperature (54 °C) to be ∼ 60 kJ mol^{-1}.[26] For **5**, a value of 45 kJ mol^{-1} for the free energy of activation for exchange was calculated from the coalescence temperature (−30 °C). The free energy of activation for phosphodiester exchange in **6** was determined to be 39 kJ mol^{-1} from its coalescence temperature of −58 °C. Although the details of the exchange mechanism are not known, one reasonable possibility is shown in Scheme 1. Here, the free diphenyl phosphate associates and undergoes terminal-to-bridged ligand exchange.

Integration of the phosphorus signals for **3** at the low-temperature limit indicates a 1:1 ratio of free-to-bound phosphate. In the spectra of **5** and **6**, however, the intensity ratio of the free phosphate is slightly greater than that of the bound one (55:45). The $\Delta G^{\ddagger}$ values for **5** and **6** were calculated from the rate constants determined at the coalescence temperatures assuming a 1:1 two-site exchange model.[26] This procedure is often used for unequally populated cases as well, since such results have been shown to be in good agreement with those

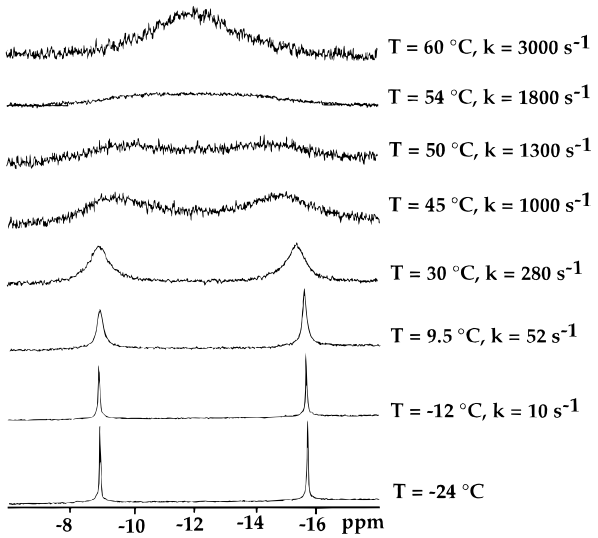

Figure 8. Variable-temperature $^{31}P\{^1H\}$ NMR spectra of **3**·CH_3OH in CD_3OD.

for a complete line shape analysis.[52] Furthermore, the values of $\Delta G^{\ddagger}$ are not highly sensitive to errors in the rate constant.[26,52] The difference in the intensity ratios for **5** and **6** suggests that some fraction of the bridging diphenyl phosphate ligand is further dissociated from the dinuclear center. This result indicates that the diphenyl phosphate ligands are more labile in the carboxylate-bridged dizinc(II) and the dicalcium(II) complexes than in the dimagnesium(II) analog (vide infra).

Relevance to Magnesium-Activated Phosphatase Enzymes. The dinuclear magnesium(II) compounds described here are structurally similar to several phosphate ester-processing metalloenzyme active sites.[1,2] Compound **1** is a possible structural model for dimagnesium-dependent metalloenzyme active sites in the absence of bound substrate. Compounds **2** and **3**, the first structurally characterized phosphate ester-bridged dimagnesium(II) complexes, are potential biomimetic models for the binding of phosphodiesters to magnesium-dependent phosphatases. The Mg···Mg separations in **2** and **3** are comparable to the corresponding distances in several phosphatase enzymes, such as ribonuclease H of HIV-1 reverse transcriptase (4 Å),[2] rat DNA polymerase β (4 Å),[3,4] and fructose-1,6-bisphosphatase (4.3 Å).[5,6] The carboxylate-bridged dimagnesium(II) compounds **1**−**3** have metal−metal distances which vary from 4.11 to 4.78 Å. This range indicates that the carboxylates in the XDK ligand can readily accommodate changes in the metal coordination environment. Such intrinsic flexibility of the carboxylate donors may help facilitate substrate binding and product release at similar carboxylate-bridged dimagnesium(II) centers in phosphate ester-processing enzymes.

Comparisons of Dimagnesium(II), Dizinc(II), and Dicalcium(II) Carboxylate-Bridged Centers. The present phosphate ester complexes afford a comparison of these metal ions in biologically relevant environments, providing a direct comparison of Mg^{2+}, Ca^{2+}, and Zn^{2+} from a biomimetic perspective.

The solid state structures of **3**, **5**, and **6** reveal some of the unique characteristics of the different metal ions. In all three, there is a dinuclear metal center bridged by the carboxylate oxygen atoms of XDK and a bidentate diphenyl phosphate ligand. In the dimagnesium(II) complex **3**, Mg1 has trigonal bipyramidal and Mg2 octahedral geometry, with the monodentate phosphate ester bound to Mg1. For the dizinc(II) analog **5**, Zn1 is tetrahedral and Zn2 octahedral, with the terminal

(51) Cohn, M.; Hughes, T. R., Jr. *J. Biol. Chem.* **1962**, *237*, 176−181.

(52) Kost, D.; Carlson, E. H.; Raban, M. *Chem. Commun.* **1971**, 656−657.

Scheme 1. Proposed Mechanism for Phosphate Ester Exchange[a]

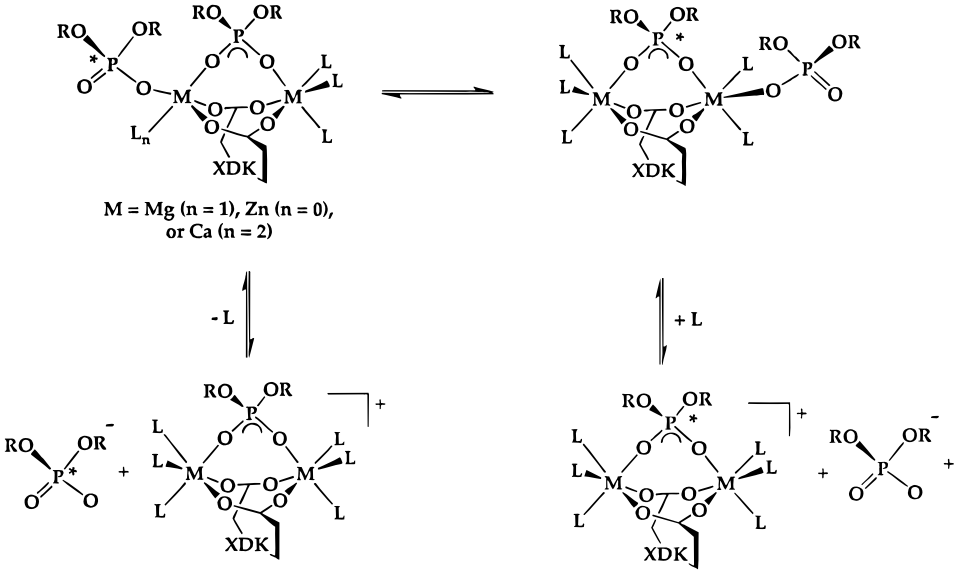

[a] M = Mg(II), Zn(II), or Ca(II); L = CD_3OD or H_2O.

diphenyl phosphate ligand being coordinated to Zn1. In the dicalcium(II) analog **6**, Ca1 and Ca2 are both octahedral, with a phosphate group bridging Ca2 and Ca1A from a neighboring molecule, leading to a polymeric structure. The results reflect the preferred coordination numbers for these metals, with calcium adopting the highest coordination number, followed by magnesium, then zinc.[50]

The metal−metal separations in **3** and **5** are comparable to the distances found in phosphatases, such as the Klenow fragment of DNA polymerase I which can accommodate $2Mg^{2+}$, $2Zn^{2+}$, or Mg^{2+}/Zn^{2+} ions in its carboxylate-bridged center at a M···M distance of 3.9 Å.[1] Interestingly, this enzyme is not activated by calcium(II).[53] The Ca···Ca distance of 4.4628(9) Å in **6** suggests that the inability of calcium(II) to activate this enzyme may be due in part to the larger metal−metal separation required for this carboxylate-bridged center.

Until recent NMR work on the C_2 domains of synaptotagmin and protein kinase C,[54] there were no examples of structurally characterized carboxylate-bridged dicalcium(II) metalloenzymes. In the C_2 domain, the Ca^{2+} ions are apparently linked by both bidentate and monodentate bridging aspartate residues. In SNase, two calcium(II) ions are required for catalysis of phosphate ester hydrolysis,[55] but in the available crystal structures, only one calcium(II) ion coordinated by two monodentate aspartate residues has been observed.[56,57] One of the monodentate aspartate residues in the active site could potentially coordinate to the other required calcium(II) ion in this enzyme. The dicalcium(II) complex **6** may be a useful structural model for biochemists studying SNase, protein kinase C, and related C_2-domain proteins, and other calcium-dependent enzymes.

Since **3**, **5**, and **6** have structural similarities to phosphate ester-processing metalloenzymes, their phosphodiester ligand exchange properties in solution were investigated. Solution studies of **3**, **5**, and **6** in methanol are consistent with the dissociation of the monodentate diphenyl phosphate ligand. The two metal ions are in equivalent environments, as evidenced by their ^1H and $^{31}P\{^1H\}$ NMR spectra. Conductivity measurements revealed 1:1 electrolyte behavior, supporting the observation of a dissociated diphenyl phosphate ligand. These results indicate that the bridging phosphate ester ligand is more stable to exchange than the terminal one.

The variable-temperature $^{31}P\{^1H\}$ NMR study revealed that the bound and free phosphodiester ligands exchange with one another in methanol. The phosphate ester exchange rates at 25 °C were calculated to be 1.9×10^2 s^{-1}, 7.5×10^4 s^{-1}, and 9.1×10^5 s^{-1}, respectively, for **3**, **5**, and **6**. Thus, the phosphate ester exchange rate of the dimagnesium(II) compound (**3**) is $\sim 10^2$ times slower than that of the dizinc(II) analog (**5**) and $\sim 10^3$ times slower than that of the dicalcium(II) complex (**6**). These relative values parallel the differences in H_2O exchange rates of hydrated magnesium(II), zinc(II), and calcium(II) ions, 10^5, 3×10^7, and $\sim 10^8$ s^{-1}, respectively.[58] The fact that the dimagnesium(II) center in **3** is kinetically less labile with respect to diphenyl phosphate ligand exchange than the dizinc(II) center in **5** and the dicalcium(II) center in **6** may be useful for understanding the metal ion preferences of phosphate ester-processing enzymes.

In the Klenow fragment of DNA polymerase I, the carboxylate-bridged dimetallic active site can employ a $2Mg^{2+}$, $2Zn^{2+}$, or a Mg^{2+}/Zn^{2+} pair. Although the identity of the metal ions in vivo has not yet been determined, the X-ray structure of the Klenow fragment complexed with a deoxynucleoside monophosphate product in the presence of both zinc and magnesium revealed a pentacoordinate Zn^{2+} ion in one site (site A) and an octahedral Mg^{2+} ion in the other (site B).[1] In the two-metal-ion phosphoryl transfer mechanism proposed for this enzyme, the metal ion in site A is postulated to generate the attacking hydroxyl ion nucleophile, and the metal ion in site B to stabilize the pentavalent phosphorus transition state. Our observation that carboxylate-bridged dimagnesium(II) centers provide a kinetically more stable binding site for phosphate esters than the corresponding dizinc(II) center is consistent with this site preference. Furthermore, our results offer some insight into the inability of calcium(II) ions to activate the Klenow fragment.

(53) Lehman, I. R.; Richardson, C. C. *J. Biol. Chem.* **1964**, *239*, 233−241.
(54) Shao, X.; Davletov, B. A.; Sutton, R. B.; Südhof, T. C.; Rizo, J. *Science* **1996**, *273*, 248−251.
(55) Cuatrecasas, P.; Fuchs, S.; Anfinsen, C. B. *J. Biol. Chem.* **1967**, *242*, 3063−3067.
(56) Cotton, F. A.; Hazen, E. E., Jr.; Legg, M. J. *Proc. Natl. Acad. Sci. U.S.A.* **1979**, *76*, 2551−2555.
(57) Loll, P. J.; Quirk, S.; Lattman, E. E.; Garavito, R. M. *Biochemistry* **1995**, *34*, 4316−4324.
(58) Eigen, M. *Pure Appl. Chem.* **1963**, *6*, 97−115.

In addition to the relatively large metal−metal separation in a dicalcium(II) carboxylate-bridged environment mentioned above, the more rapid phosphate ester exchange rate may be too fast to bind and orient the substrate properly.

The faster rate of phosphate ester exchange for the dicalcium(II) complex (**6**) may be useful in explaining the metal ion preferences of SNase. This highly proficient calcium-dependent enzyme accelerates the hydrolysis of phosphodiester bonds by a factor of 10^{16}.[59] Other metal ions such as Co^{2+} and Mn^{2+} bind competitively at the Ca^{2+} binding site, but are at least 10^5-fold less effective at activating the enzyme.[60] Magnesium(II) ions have been reported to be ineffective at activating this enzyme,[61] and zinc(II) is a potent inhibitor.[62] The rate-determining step for SNase is believed to be product release.[63] Our results that carboxylate-bridged dicalcium(II) centers exchange phosphate esters more rapidly than dimagnesium(II) and dizinc(II) analogs are consistent with the preference of SNase for calcium(II).

Conclusions

With the use of the dinucleating XDK ligand, we have prepared several novel carboxylate-bridged dimagnesium(II) complexes, which are potential biomimetic models for phosphate ester-processing metalloenzymes. These magnesium(II) complexes should be of value for interpreting electron density maps in protein X-ray crystal structure determinations, since the current resolution of many dimagnesium-dependent metalloenzymes structures is too low to reveal detailed geometries around the metal center. The dinuclear magnesium−XDK center is unstable in the presence of acid, however, as evidenced by protonation of the carboxylate ligand to liberate one magnesium(II) ion and generate $[Mg(HXDK)_2(H_2O)_2]$ (**4**).

The carboxylate- and phosphodiester-bridged magnesium, zinc, and calcium complexes are useful models for studying the behavior of these metal ions in relevant biomimetic environments. The metal−metal separation in the dimagnesium and the dizinc complexes are comparable to those found in similar carboxylate-bridged phosphatase active sites. The observed differences in phosphate ester exchange rates for dimagnesium, dizinc, and dicalcium centers were found to be comparable to the differences in water exchange rates for the hydrated metal ions. The phosphodiester exchange rates may be useful to biochemists studying phosphate ester-processing metalloenzymes. Elsewhere we describe the functional activity of the phosphatase model complexes.

Acknowledgment. This work was supported by a grant from the National Science Foundation. T.T. is grateful to the Shigaku Shinko Zaidan for an International Research Fellowship.

Supporting Information Available: Tables of complete atomic positional and anisotropic thermal parameters, bond lengths, and angles for **1**(NO_3), **2**·$3CH_3OH$, **3**·CH_3OH, **4**, and **6**·CH_3OH, and a figure showing the atomic numbering scheme of the XDK ligand (45 pages). Ordering information is given on any current masthead page.

IC960894H

(59) Radzicka, A.; Wolfenden, R. *Science* **1995**, *267*, 90−93.
(60) Serpersu, E. H.; Shortle, D.; Mildvan, A. S. *Biochemistry* **1987**, *26*, 1289−1300.
(61) Cunningham, L.; Catlin, B. W.; Privat de Garilhe, M. *J. Am. Chem. Soc.* **1956**, *78*, 4642−4645.
(62) Cuatrecasas, P.; Fuchs, S.; Anfinsen, C. B. *J. Biol. Chem.* **1961**, *242*, 1541−1547.
(63) Hale, S. P.; Poole, L. B.; Gerlt, J. A. *Biochemistry* **1993**, *32*, 7479−7487.